TOPOLOGY OPTIMIZATION ALGORITHM USING TWO-POINT TOPOLOGICAL DERIVATIVE

Masaki NODA[1)], Kei MATSUSHIMA[2)] and Takayuki YAMADA[3)]

1)The University of Tokyo (〒 113-8656 2-11-16, Yayoi, Bunkyo, Tokyo, Japan, E-mail: noda-masaki442@g.ecc.u-tokyo.ac.jp)
2)The University of Tokyo (〒 113-8656 2-11-16, Yayoi, Bunkyo, Tokyo, Japan, E-mail: matsushima@mech.t.u-tokyo.ac.jp)
3)The University of Tokyo (〒 113-8656 2-11-16, Yayoi, Bunkyo, Tokyo, Japan, E-mail: t.yamada@mech.t.u-tokyo.ac.jp)

This paper proposes a topology optimization method that employs the two-point topological derivative as the sensitivity. The sensitivity evaluates the sensitivity of an objective functional relative to the generation of a thin bar connecting two distant portions of a boundary. Using this topological derivative, a topology optimization method is constructed based on the level set method. The proposed method drastically reduces the likelihood of local optima in topology optimization processes. Several numerical examples are given to demonstrate the effectiveness of the proposed method.

Key Words: Topological ligament, Two-point topological derivative, Topology optimization, Level set method, Structural optimization, Finite element method

1. Introduction

The topological derivative[(1–4)] is the sensitivity to emergence of a small hole in the internal domain of a structure, which can cause changes in the external shape and the topology, i.e., the presence or absence of a hole, in a structural optimization problem. This can allow drastic improvement of structural performance.

Beginning with the bubble method proposed by Eschenauer et al. to handle the drawbacks of an unchanged topology in shape optimization[(5)], topology optimization using topological derivatives has been studied actively for elasticity and other problems[(6–14)].

However, this sensitivity has a severe drawback when applied to some physics problems (e.g., elasticity and heat conduction), i.e., the sensitivity is uniformly zero inside a void domain because a small floating island of structural material in the void domain does not improve the stiffness, strength, or conductivity of the overall structure. When an iterative optimization process is performed using this sensitivity, material construction is not promoted inside a void domain. Therefore, domains that are void in the initial design are likely to be void in the final design, i.e., the optimized design is highly dependent on the initial design.

In contrast, in the ground structure method [(15–17)], the dimension and presence or absence of each beam of a truss or rigid frame structure is optimized. This method employs the sensitivity to generate a new beam connecting two distant nodes.

In analogy with this method, in this paper, we utilize a bar generating topological derivative that generates a new bar connecting a portion of the boundary of the void domain with a distant portion of the boundary. This sensitivity to generate a bar can be generalized for the generation of arbitrary curvilinear ligaments[(18)]. The sensitivity is called an external topological derivative, topological ligament, or two-point topological derivative. This sensitivity is utilized in shape optimization[(19)] and layout optimization[(20)]. As shown in previous studies, the use of two-point topological derivative for structural optimization further promotes structural changes. That is, not only does the external shape changes or emerges in the structural domain, but the cavity domain is split into two parts by the structural material domain. By these drastic changes in structure, the highest performance structure is more likely to be obtained.

In this study, we utilize the two-point topological derivative in topology optimization. While shape optimization only changes the external shape during the optimization pro-

Recieved 2022, Oct., 27, accepted 2022, Nov., 21

cess, topology optimization generates new holes, which leads to a better solution. The use of two-point topological derivative in conjunction with conventional single-point topological derivative promotes further drastic structural changes, which can lead to performance improvements.

The remainder of this paper is organized as follows. Section 2 describes the general topology optimization problem. In Section 3, we describe the formulation of two-point topological derivative. In Section 4, a topology optimization method is constructed using the two-point topological derivative. In Section 5, the proposed method is applied to the linear elasticity problem, and a sensitivity analysis is discussed. This sensitivity is validated in a numerical framework in Section 6, and several numerical examples are given in Section 7 to demonstrate the effectiveness of the proposed method. Finally, the paper is concluded in Section 8.

2. Topology optimization problem

Based on the level set method, the topology optimization problem is generally formulated as follows:

$$\min_{\phi, u(\phi)} \; J(\phi, u),$$

$$\text{subject to} \begin{cases} \phi(\mathbf{x}) > 0 \quad \text{for} \;\; \mathbf{x} \in \Omega \\ \text{Governing Equations for} \;\; u(\Omega) \\ G_i(\Omega, u) \leq 0 \;\; \text{for} \;\; i \in \{1, \ldots, n_G\} \\ H_j(\Omega, u) = 0 \;\; \text{for} \;\; j \in \{1, \ldots, n_H\} \end{cases}, \qquad (1)$$

where the scalar function $\phi(\mathbf{x})$ $(\mathbb{R}^d \to \mathbb{R}, d \in \{2, 3\})$ is the level set function that defines the structural domain $\Omega \subset \mathbb{R}^d$, u is the state variable, J is the objective functional, G_i are inequality constraint functions, H_j are equality constraint functions, and n_G and n_H are the number of constraints.

3. Definition of two-point topological derivative

Here, we consider the domain of a thin bar $\Omega^{\text{bar}}(w, \mathbf{x}_1, \mathbf{x}_2)$ that connects a portion of the boundary of the void domain $\mathbf{x}_1 \in \partial\Omega$ to a distant portion of the boundary $\mathbf{x}_2 \in \partial\Omega$ (Fig. 1). As can be seen, the bar has a uniform cross-sectional shape (or uniform width) whose cross-sectional area (or width) is w. We assume that this bar does not intersect the structural domain $\forall\beta \in (0, 1), \mathbf{x}_1 + \beta(\mathbf{x}_2 - \mathbf{x}_1) \notin \Omega$, which means that the pairs of coordinates $\mathbf{x}_1'$ and $\mathbf{x}_2'$ shown in Fig. 2 are excluded.

Then, we consider a topological change in which a new bar is generated in the void domain. The two-point topological derivative $\mathcal{D}^2 J(\mathbf{x}_1, \mathbf{x}_2)$, which is a sensitivity to the topology changes of generating a new bar, is defined as follows:

$$\mathcal{D}^2 J(\mathbf{x}_1, \mathbf{x}_2) = \lim_{w \to 0} \frac{J(\Omega \cup \Omega^{\text{bar}}(w, \mathbf{x}_1, \mathbf{x}_2)) - J(\Omega)}{\text{meas}(\Omega^{\text{bar}}(w, \mathbf{x}_1, \mathbf{x}_2))}, \qquad (2)$$

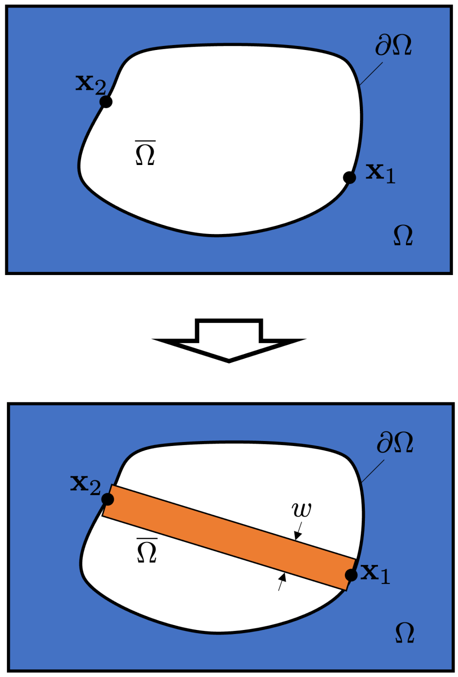

Fig. 1 Generating a bar domain.

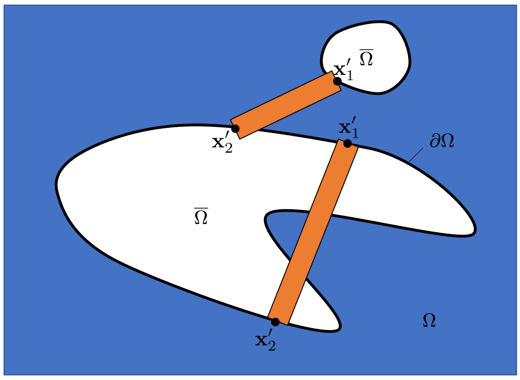

Fig. 2 Excluded pairs of coordinates.

where $\text{meas}(\Omega^{\text{bar}})$ is the measure of the domain Ω^{bar}.

4. Construction of a topology optimization method utilizing two-point topological derivative

In this section, we describe the construction of an iterative topology optimization algorithm driven by the two-point topological derivative $\mathcal{D}^2 J(\mathbf{x}_1, \mathbf{x}_2)$.

The topology optimization problem given in Eq. (1) is difficult to solve directly; thus, we assume an initial value of the level set function and update it using the topological derivatives as follows:

$$\phi'(\mathbf{x}) + \tau \nabla^2 \phi'(\mathbf{x}) = \phi^{\text{old}}(\mathbf{x}) - K \times \begin{cases} \mathcal{D}^1 J(\mathbf{x}) & \text{for } \mathbf{x} \in \Omega \\ h\overline{\mathcal{D}^2} J(\mathbf{x}) & \text{for } \mathbf{x} \notin \Omega \end{cases}, \qquad (3)$$

$$\phi = \min\{1, \max\{-1, \phi'\}\}, \qquad (4)$$

where the second term on the left side of Eq. (3) is a regularization term used to obtain a smooth optimal structure(21), τ is a regularization factor which can adjust the geometrical complexity(21), K is a coefficient to adjust the change of the design variable ϕ in one step, and $\mathcal{D}^1 J$ is the conventional single point topological derivative, which leads to emergence of a new hole. h is a small positive number, which is set to 0.1 in this study. This means that the bar domain is generated only in domains where it is very useful to improve the objective function. The closer this value h is to 1, the easier it is to avoid local optimums, but instead, problems arise such as repeated appearance and disappearance of bar domains, or the spread of domains where the value of the level set function ϕ is around 0. Note that Eq. (4) limits the level set function to concentrate the effect of regularization term near the boundary, and the sensitivity $\overline{\mathcal{D}^2} J(\mathbf{x})$ is the solution of the following problem:

$$\overline{\mathcal{D}^2} J(\mathbf{x}) = \min_{\mathbf{x}_1, \mathbf{x}_2 \in \partial\Omega} \mathcal{D}^2 J(\mathbf{x}_1, \mathbf{x}_2), \tag{5}$$

$$\text{subject to} \begin{cases} \exists \alpha \in (0,1), \mathbf{x} = \mathbf{x}_1 + \alpha(\mathbf{x}_2 - \mathbf{x}_1) \\ \forall \beta \in (0,1), \mathbf{x}_1 + \beta(\mathbf{x}_2 - \mathbf{x}_1) \notin \Omega \end{cases}. \tag{6}$$

Here, the constraints mean that coordinate $\mathbf{x}$ is in the bar, and the bar does not intersect the structural domain Ω. In addition, from the constraints, there exists at most one $\mathbf{x}_2$ corresponding to $\mathbf{x}$ and $\mathbf{x}_1$.

5. Compliance minimization problem

In this section, the proposed method is applied to the following compliance minimization problem with a volume constraint:

$$\min_{\phi, u} \ J(u) = \int_{\Gamma^{\text{in}}} \mathbf{t} \cdot \mathbf{u} \mathrm{d}\Gamma,$$

$$\text{subject to} \begin{cases} \phi(\mathbf{x}) > 0 \quad \text{for} \ \ \mathbf{x} \in \Omega \\ \int_\Omega \varepsilon(\mathbf{u}) : C : \varepsilon(\mathbf{v}) \mathrm{d}\mathbf{x} = \int_{\Gamma^{\text{in}}} \mathbf{t} \cdot \mathbf{v} \mathrm{d}\Gamma \\ \mathbf{u} = \mathbf{0} \ \ \text{on} \ \Gamma^{\text{fix}} \\ G(\Omega) = \int_\Omega \mathrm{d}\mathbf{x} - \hat{V} \leq 0 \end{cases}, \tag{7}$$

where $\mathbf{t}$ is a traction force vector, $\varepsilon(\mathbf{u})$ is the strain tensor of $\mathbf{u}$, whose i, j component is $\varepsilon_{ij}(\mathbf{u}) = \frac{1}{2} (\partial u_i / \partial x_j + \partial u_j / \partial x_i)$, C is the elastic modulus tensor, $\mathbf{v}$ is the test function, Γ^{fix} is a boundary with displacement defined as zero, and $\hat{V}$ is the maximum volume. The conventional topological derivative, which lead to a emergence of a new hole, is computed as follows:

$$\mathcal{D}^1 J(\mathbf{x}) = \varepsilon(\mathbf{u}(\mathbf{x})) : A : \varepsilon(\mathbf{u}(\mathbf{x})), \tag{8}$$

where A is the elastic moment tensor(3).

Here, we evaluate the two-point topological derivative $\mathcal{D}^2 J(\mathbf{x}_1, \mathbf{x}_2)$ introduced in Section 3. First, we assume that the displacement field in the presence of an infinitely thin bar domain is approximately equal to the displacement field in the absence of that bar domain. Then, we have

$$\tilde{\mathbf{u}}(\Omega) \equiv \mathbf{u}(\Omega \cup \Omega^{\text{bar}}(w, \mathbf{x}_1, \mathbf{x}_2)) \simeq \mathbf{u}(\Omega). \tag{9}$$

The above assumption is expected to hold for the generation of thin bars, which is the target of this study. However, if there are Dirichlet or inhomogeneous Neumann boundary conditions at the boundaries of the newly generated domain, or if the structural domain is divided by a thin void domain rather than a bar being generated in a cavity, the above assumption is not valid, and an appropriate evaluation is required.

In addition, we assume that the stress fields are approximately uniform around the thin bar domain.

The generated element supports only an axial force like a bar element. In this case, the axial elasticity modulus $k(w, \mathbf{x}_1, \mathbf{x}_2)$ can be computed using Young's modulus E as follows:

$$k(w, \mathbf{x}_1, \mathbf{x}_2) = \frac{Ew}{|\mathbf{x}_1 - \mathbf{x}_2|}. \tag{10}$$

Thus, the additional strain energy for $\Omega^{\text{bar}}(w, \mathbf{x}_1, \mathbf{x}_2)$, i.e., the change of compliance J, can be computed approximately as follows:

$$\begin{aligned} & J(\Omega \cup \Omega^{\text{bar}}(w, \mathbf{x}_1, \mathbf{x}_2)) - J(\Omega) \\ =& \int_{\Omega \cup \Omega^{\text{bar}}(w, \mathbf{x}_1, \mathbf{x}_2)} \varepsilon(\tilde{\mathbf{u}}) : C : \varepsilon(\tilde{\mathbf{u}}) \mathrm{d}\mathbf{x} - \int_\Omega \varepsilon(\mathbf{u}) : C : \varepsilon(\mathbf{u}) \mathrm{d}\mathbf{x} \\ \simeq& \int_{\Omega^{\text{bar}}(w, \mathbf{x}_1, \mathbf{x}_2)} \varepsilon(\tilde{\mathbf{u}}) : C : \varepsilon(\tilde{\mathbf{u}}) \mathrm{d}\mathbf{x} \\ \simeq& \int_{\Omega^{\text{bar}}(w, \mathbf{x}_1, \mathbf{x}_2)} \varepsilon(\mathbf{u}) : C : \varepsilon(\mathbf{u}) \mathrm{d}\mathbf{x} \\ \simeq& k(w, \mathbf{x}_1, \mathbf{x}_2) \left((\mathbf{u}(\mathbf{x}_1) - \mathbf{u}(\mathbf{x}_2)) \cdot \frac{(\mathbf{x}_1 - \mathbf{x}_2)}{|\mathbf{x}_1 - \mathbf{x}_2|} \right)^2. \end{aligned} \tag{11}$$

In addition, the measure of domain $\Omega^{\text{bar}}(w, \mathbf{x}_1, \mathbf{x}_2)$ is computed as follows:

$$\text{meas}(\Omega^{\text{bar}}(w, \mathbf{x}_1, \mathbf{x}_2)) = w|\mathbf{x}_1 - \mathbf{x}_2|. \tag{12}$$

Thus, the two-point topological derivative can be computed approximately as follows:

$$\mathcal{D}^2 J(\mathbf{x}_1, \mathbf{x}_2) = \frac{E((\mathbf{u}(\mathbf{x}_1) - \mathbf{u}(\mathbf{x}_2)) \cdot (\mathbf{x}_1 - \mathbf{x}_2))^2}{|\mathbf{x}_1 - \mathbf{x}_2|^4}. \tag{13}$$

See previous studies for more detailed derivation(20, 22).

5.1. Numerical implementation and computational cost

The sensitivity $\overline{\mathcal{D}^2} J(\mathbf{x})$ is calculated as follows. Initialize the value $\overline{\mathcal{D}^2} J(\mathbf{x})$ for each node as sufficiently large value.

Let $\mathcal{E}$ be the set of edges over the boundary of the domain Ω. Let $\mathcal{N}$ be the set of nodes that belong to these edges $\mathcal{E}$. For every triangles consisting of edge j in $\mathcal{E}$ and two edges, which connect the node i in $\mathcal{N}$ and the both ends of edge j, search the nodes in the triangle and label them as $\mathcal{N}_{ij}$. If all the nodes in $\mathcal{N}_{ij}$ belong to the void, i.e., $\phi < 0$, then calculate the sensitivity $\mathcal{D}^2 J(\mathbf{x}^i, \mathbf{x}^{j1})$ and $\mathcal{D}^2 J(\mathbf{x}^i, \mathbf{x}^{j2})$, where $\mathbf{x}^i$ is the coordinate of the node i and $\mathbf{x}^{j1}$ and $\mathbf{x}^{j2}$ are the coordinate of nodes which belong to the edge j. For each node l in $\mathcal{N}_{ij}$, calculate $\mathcal{D}^2 J(\mathbf{x}^i, \mathbf{x}^*)$ by interpolation using $\mathcal{D}^2 J(\mathbf{x}^i, \mathbf{x}^{j1})$ and $\mathcal{D}^2 J(\mathbf{x}^i, \mathbf{x}^{j2})$, where $\mathbf{x}^*$ is the coordinate that satisfies the constraint Eq. (6). If the value $\mathcal{D}^2 J(\mathbf{x}^i, \mathbf{x}^{j2})$ is smaller than $\overline{\mathcal{D}^2} J(\mathbf{x}^l)$, then substitute the value, where $\mathbf{x}^l$ is the coordinate of node l.

In the following, we assess the computational cost of computing $\overline{\mathcal{D}^2} J$ for each optimization step. Here, let n be the number of nodes on a finite element mesh. Then, the number of nodes or edges on the boundary of voids is given as $\mathcal{O}(n^{(d-1)/d})$. Thus, from the above calculation scheme, the computational complexity of computing $\overline{\mathcal{D}^2} J$ is at most $\mathcal{O}(n^{(d-1)/d}) \times \mathcal{O}(n^{(d-1)/d}) \times \mathcal{O}(n) = \mathcal{O}(n^2)$ or $\mathcal{O}(n^{7/3})$.

Since this calculation is computationally time-consuming, we may choose appropriate steps to calculate it instead of doing it for all optimization steps; however, in this study, we simply did this calculation for all optimization steps.

6. Numerical validation of sensitivity analysis

The analytical formula for the two-point topological derivative given in Eq. (13) can be validated using the following computational framework.

Here for a finite value of ε, we define a numerical difference $\mathcal{D}^2_\varepsilon J(\mathbf{x}_1, \mathbf{x}_2)$ as follows:

$$\mathcal{D}^2_\varepsilon J(\mathbf{x}_1, \mathbf{x}_2) = \frac{J(\Omega + \Omega^{\mathrm{bar}}(\varepsilon, \mathbf{x}_1, \mathbf{x}_2)) - J(\Omega)}{\mathrm{meas}(\Omega^{\mathrm{bar}}(\varepsilon, \mathbf{x}_1, \mathbf{x}_2))}. \qquad (14)$$

Under the two-dimensional linear elastic condition shown in

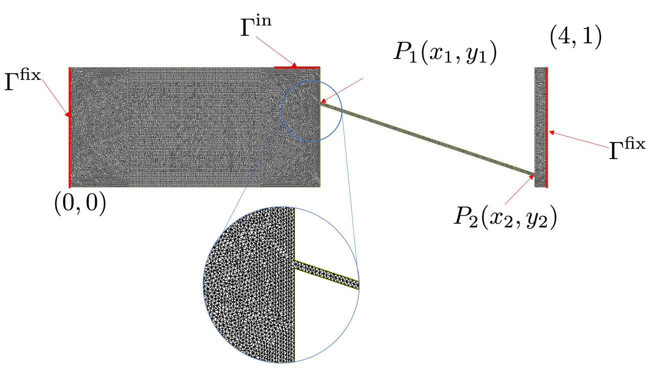

Fig. 3 Domain and conditions for numerical validation of sensitivity analysis.

Fig. 3 with traction force $\mathbf{t} = (0, -1)^T$ and Young's modulus $E = 200$ [GPa], with the finite element method, the numerically approximated values are calculated for $J(\Omega)$ and

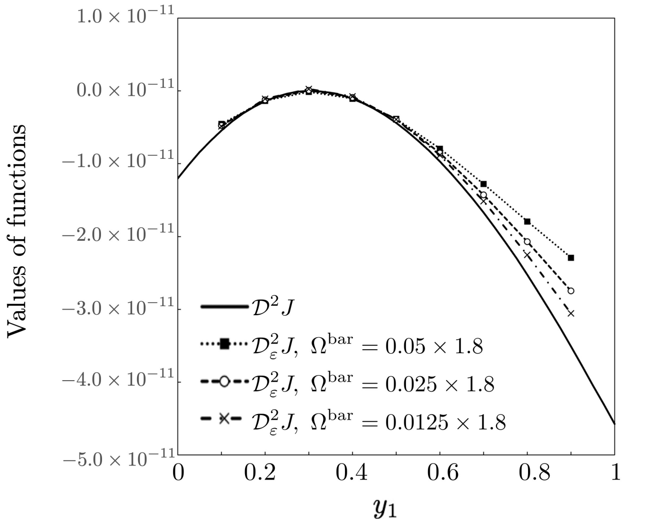

Fig. 4 Results of numerical validation of sensitivity analysis

$J(\Omega + \Omega^{\mathrm{bar}}(\varepsilon, \mathbf{x}_1, \mathbf{x}_2))$ for each bar of the area $\mathrm{meas}(\Omega^{\mathrm{bar}}(\varepsilon, \mathbf{x}_1, \mathbf{x}_2)) \in \{0.0125 \times 1.8, 0.025 \times 1.8, 0.05 \times 1.8\}$ connecting coordinate $\mathbf{x}_1 \in \{(2.1, 0.1)^T, (2.1, 0.2)^T, \ldots, (2.1, 0.9)^T\}$ to $\mathbf{x}_2 = (3.9, 0.1)^T$.

In addition, the analytical value $\mathcal{D}^2 J(\mathbf{x}_1, \mathbf{x}_2)$ for the state variables where there is no bar $\mathbf{u}(\Omega)$ is calculated for $\mathbf{x}_1 = (2.1, y_1)^T$, $y_1 \in [0, 1]$ and $\mathbf{x}_2 = (3.9, 0.1)^T$.

The values of $\mathcal{D}^2 J(\mathbf{x}_1, \mathbf{x}_2)$ and $\mathcal{D}^2_\varepsilon J(\mathbf{x}_1, \mathbf{x}_2)$ are plotted in Fig. 4. As can be seen, the values of $\mathcal{D}^2_\varepsilon J(\mathbf{x}_1, \mathbf{x}_2)$ are approximately consistent and become closer to the values of $\mathcal{D}^2 J(\mathbf{x}_1, \mathbf{x}_2)$ as the area $\mathrm{meas}(\Omega^{\mathrm{bar}}(\varepsilon, \mathbf{x}_1, \mathbf{x}_2))$ becomes smaller. This confirms the usefulness of the analytical formula given in Eq. (13).

7. Numerical examples

In this section, we provide several numerical examples to demonstrate the effectiveness of the proposed method.

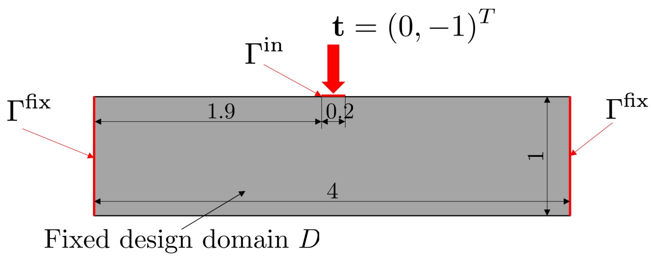

Fig. 5 Domain and boundary conditions for condition 1.

In these examples, the elastic modulus of the structural material is set to $E = 200$ [GPa] and the external domain of the fixed design domain $D \subset \mathbb{R}^d$ is assumed to be void. To avoid numerical instability, the void domain internal fixed design domain $\overline{\Omega} \cap D$ is given Young's modulus $E = 0.1$ [GPa].

Figure 5 shows the calculation condition 1. In this condition, the upper limit of the volume is set to $\hat{V} = 1.2$ [m^2],

(a) Initial distribution of level set function ϕ (b) Conventional single-point topological derivative $\mathcal{D}^1 J$ for initial design (c) Sensitivity $\overline{\mathcal{D}^2} J$ for initial design

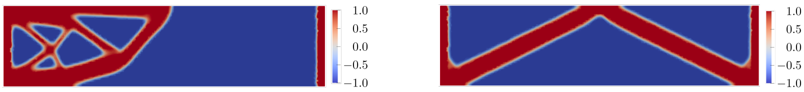

(d) The optimized distribution of ϕ when only single-point topological derivative is used (the compliance is 12.4×10^{-12}). (e) The optimized distribution of ϕ when both the single-point and two-point topological derivatives are used (the compliance is 5.36×10^{-12}).

Fig. 6 Initial design, topological derivatives and optimized designs for condition 1.

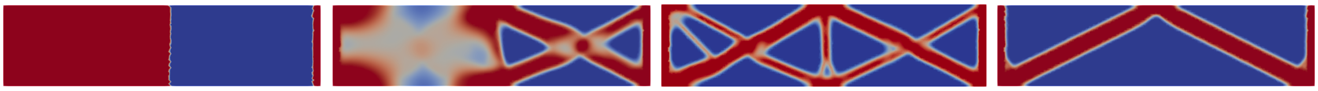

(a) case 1, step 0 (b) case 1, step 20 (c) case 1, step 50 (d) case 1, obtained shape

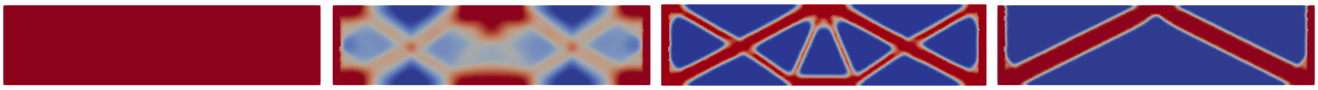

(e) case 2, step 0 (f) case 2, step 20 (g) case 2, step 50 (h) case 2, obtained shape

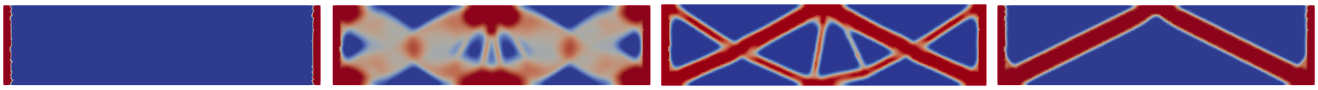

(i) case 3, step 0 (j) case 3, step 20 (k) case 3, step 50 (l) case 3, obtained shape

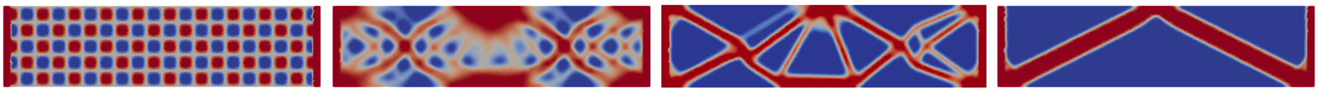

(m) case 4, step 0 (n) case 4, step 20 (o) case 4, step 50 (p) case 4, obtained shape

Fig. 7 Dependency on initial configurations.

and the left and right side 0.1 [m] of D is fixed to structural material domain. As shown in Fig. 6(a), a design of left half consisted of structural material is set as initial design.

As shown in Fig. 6(c), two-point topological derivative has a sensitivity to generate a new bar from upper center point to lower right point. However, the single-point topological derivative has only a sensitivity to leave necessary structural parts, as can be seen in Fig. 6(b). Thus, as shown in Fig. 6(e), the optimized configuration according to the proposed method is a double-ended support beam, which is considered to be structurally appropriate. In contrast, the optimized configuration according to ordinal topology optimization (Fig. 6(d)) is a cantilever depending on the initial design. With the features of the structure, the value of the objective function obtained by the proposed method is less than half that of the conventional method. This indicates that better performance is obtained using the proposed method.

Figs. 7(a)–7(d) shows the distribution of the level set function in the optimization process. Figs. 7(e),7(i), and 7(m) show the other initial designs. Figs. 7(f)–7(h),7(j)–7(l), and 7(n)–7(p) show the optimization results. It can be seen that the same optimal configurations are obtained.

Fig. 8(a) shows the domain and boundary conditions for the condition 2. In this condition, the upper limit of the volume is set to $\hat{V} = 0.9$ [m^2], and the left and upper side 0.1 [m] of D is fixed to structural material domain. Fig. 8(b) shows the initial design. Fig. 8(c) shows the design obtained by only the single-point topological derivative. Fig. 8(d) shows the design obtained by proposed method. In the design obtained by proposed method, the upper fixed boundary and the load boundary are directly connected by the structural material, and the compliance value is improved by a factor of 10.

8. Conclusion

This paper has proposed a topology optimization method, which uses the two-point topological derivative. Since the two-point topological derivative is a sensitivity to the topological changes to generate a new bar connecting two points

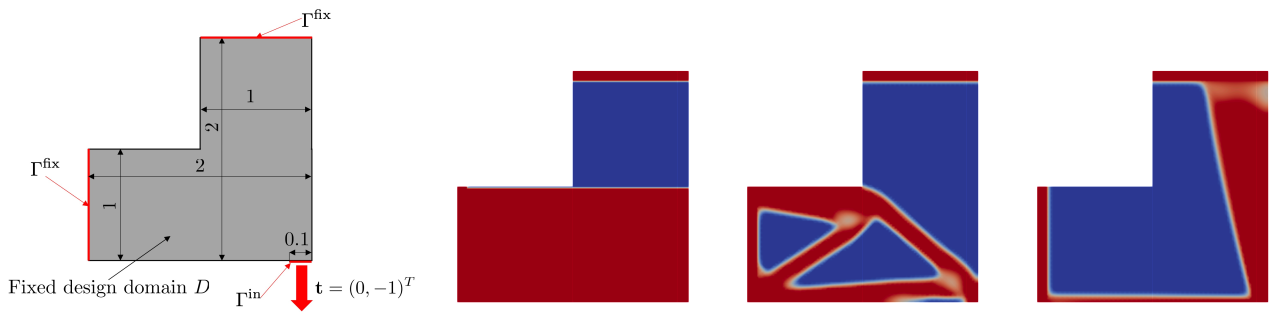

(a) Domain and boundary conditions.

(b) Initial distribution of level set function ϕ.

(c) The optimized distribution of ϕ when only single-point topological derivative is used (the compliance is 4.0×10^{-12}).

(d) The optimized distribution of ϕ when both the single-point and two-point topological derivatives are used (the compliance is 3.8×10^{-13}).

Fig. 8 Optimization settings and results for condition 2.

of boundary, the proposed method can significantly reduce the problem of local optimum problem. Several numerical examples were given under the condition that conventional method are prone to local optimum solutions depending on the initial design. The results confirm the effectiveness of the proposed method.

Acknowledgment

This work was supported by JST FOREST Program (Grant Number JPMJFR202J, Japan).

The authors would like to thank Enago (www.enago.jp) for the English language review.

References

(1) J. Sokolowski, A. Zochowski, On the topological derivative in shape optimization, SIAM Journal on Control and Optimization 37 (4) (1999) 1251–1272. doi:10.1137/S0363012997323230.

(2) A. A. Novotny, R. A. Feijóo, E. Taroco, C. Padra, Topological sensitivity analysis, Computer methods in applied mechanics and engineering 192 (7-8) (2003) 803–829.

(3) M. Bonnet, G. Delgado, The topological derivative in anisotropic elasticity, Quarterly Journal of Mechanics and Applied Mathematics 66 (4) (2013) 557–586.

(4) G. Delgado, M. Bonnet, The topological derivative of stress-based cost functionals in anisotropic elasticity, Computers & Mathematics with Applications 69 (10) (2015) 1144–1166. doi:10.1016/j.camwa.2015.03.010.

(5) H. A. Eschenauer, V. V. Kobelev, A. Schumacher, Bubble method for topology and shape optimization of structures, Structural and Multidisciplinary Optimization 8 (1) (1994) 42–51.

(6) J. Céa, S. Garreau, P. Guillaume, M. Masmoudi, The shape and topological optimizations connection, Computer methods in applied mechanics and engineering 188 (4) (2000) 713–726.

(7) S. Garreau, P. Guillaume, M. Masmoudi, The topological asymptotic for pde systems: the elasticity case, SIAM journal on control and optimization 39 (6) (2001) 1756–1778.

(8) M. Burger, B. Hackl, W. Ring, Incorporating topological derivatives into level set methods, Journal of computational physics 194 (1) (2004) 344–362.

(9) S. Amstutz, H. Andrä, A new algorithm for topology optimization using a level-set method, Journal of computational physics 216 (2) (2006) 573–588.

(10) O. Sigmund, K. Maute, Topology optimization approaches, Structural and Multidisciplinary Optimization 48 (6) (2013) 1031–1055.

(11) H. Isakari, K. Kuriyama, S. Harada, T. Yamada, T. Takahashi, T. Matsumoto, A topology optimisation for three-dimensional acoustics with the level set method and the fast multipole boundary element method, Mechanical Engineering Journal 1 (4) (2014) CM0039–CM0039.

(12) C. G. Lopes, A. A. Novotny, Topology design of compliant mechanisms with stress constraints based on the topological derivative concept, Structural and Multidisciplinary Optimization 54 (4) (2016) 737–746.

(13) N. Kishimoto, K. Izui, S. Nishiwaki, T. Yamada, Optimal design of electromagnetic cloaks with multiple dielectric materials by topology optimization, Applied Physics Letters 110 (20) (2017) 201104.

(14) M. Noda, Y. Noguchi, T. Yamada, Extended level set method: A multiphase representation with per-

fect symmetric property, and its application to multi-material topology optimization, Computer Methods in Applied Mechanics and Engineering 393 (2022) 114742. doi:10.1016/j.cma.2022.114742.

(15) W. Dorn, Automatic design of optimal structures, J. de Mecanique 3 (1964) 25–52.

(16) P. Pedersen, On the optimal layout of multi-purpose trusses, Computers & Structures 2 (5-6) (1972) 695–712.

(17) T. Zegard, G. H. Paulino, Grand—ground structure based topology optimization for arbitrary 2d domains using matlab, Structural and Multidisciplinary Optimization 50 (5) (2014) 861–882.

(18) S. A. Nazarov, J. Sokolowski, The topological derivative of the dirichlet integral under formation of a thin ligament, Siberian Mathematical Journal 45 (2) (2004) 341–355.

(19) C. Dapogny, The topological ligament in shape optimization: a connection with thin tubular inhomogeneities, SMAI Journal of Computational Mathematics 7 (2021) 185–266.

(20) M. H. Kobayashi, R. A. Canfield, R. M. Kolonay, On a cellular developmental method for layout optimization via the two-point topological derivative, Structural and Multidisciplinary Optimization 64 (4) (2021) 2343–2360.

(21) T. Yamada, K. Izui, S. Nishiwaki, A. Takezawa, A topology optimization method based on the level set method incorporating a fictitious interface energy, Computer Methods in Applied Mechanics and Engineering 199 (45-48) (2010) 2876–2891. doi:10.1016/j.cma.2010.05.013.

(22) S. A. Nazarov, A. S. Slutskij, J. Sokolowski, Topological derivative of the energy functional due to formation of a thin ligament on a spatial body, Folia Mathematicae, Acta Universitatis Lodziensis 12 (2005) 39–72.